This is an *Accepted Manuscript*, which has been through the Royal Society of Chemistry peer review process and has been accepted for publication.

Accepted Manuscripts are published online shortly after acceptance, before technical editing, formatting and proof reading. Using this free service, authors can make their results available to the community, in citable form, before we publish the edited article. We will replace this *Accepted Manuscript* with the edited and formatted *Advance Article* as soon as it is available.

You can find more information about *Accepted Manuscripts* in the **Information for Authors**.

Please note that technical editing may introduce minor changes to the text and/or graphics, which may alter content. The journal's standard **Terms & Conditions** and the **Ethical guidelines** still apply. In no event shall the Royal Society of Chemistry be held responsible for any errors or omissions in this *Accepted Manuscript* or any consequences arising from the use of any information it contains.

www.rsc.org/materialsA

Journal of
Materials Chemistry A

ARTICLE

Enhanced Performance of Quasi-Solid-State Dye-Sensitized Solar Cells by Tuning the Building Blocks in D-(π)-A'-π-A Featured Organic Dyes

Tian Lan, Xuefeng Lu, Lu Zhang, Yijing Chen, Gang Zhou,* and Zhong-Sheng Wang

A series of D-(π)-A'-π-A featured organic dyes with different numbers of 3,4-ethylenedioxythiophene (EDOT) bridge and different anchoring groups, i.e., cyanoacrylic acid or rhodanine-3-acetic acid, have been designed and synthesized for application in quasi-solid-state dye-sensitized solar cells (DSSCs). The absorption, electrochemical and photovoltaic properties are systematically investigated. Upon the incorporation of an auxiliary EDOT unit into sensitizers **FNE60** and **FNE61** with D-A'-π-A configuration, sensitizers **FNE62** and **FNE63** with D-π-A'-π-A configuration exhibit much broader absorption spectra, which is beneficial to the light-harvesting capability and photocurrent generation. When the cyanoacrylic acid group in sensitizers **FNE60** and **FNE62** is replaced by a much stronger electron-withdrawing group, rhodanine-3-acetic acid, strengthened intramolecular charge transfer interactions are realized, which results in the significantly bathochromically shifted maximum absorption wavelengths for sensitizers **FNE61** and **FNE63**. However, the methylene group in the rhodanine-3-acetic acid unit interrupts the LUMO delocalization on the anchoring group in sensitizers **FNE61** and **FNE63**, as revealed by theoretic calculation, which may result in less effective electron injection from LUMO to the conduction band of the titania semiconductor. Consequently, the quasi-solid-state DSSC based on **FNE62** exhibits a highest power conversion efficiency of 8.2%, which illustrates good long-term stability after continuous light soaking for 1000 h.

Introduction

Dye-sensitized solar cells (DSSCs),[1] regarded as one of the most promising photovoltaic devices, have been extensively investigated due to their high theoretical efficiency, facile fabrication processes, and potential low cost. Undoubtedly, the sensitizers are considered as one of the key components in these cells since they absorb the sunlight, thereby inject excited electrons into the conduction band of nanostructured/porous titania, and then are regenerated by the electrolyte. In the past two decades, organometallic dyes of ruthenium polypyridine have been demonstrated as light-harvesters for highly efficient DSSCs, such as N719[2] and black dye,[3] which have become the most representative DSSC sensitizers with overall power conversion efficiencies (η) of over 11%. Recently, zinc-porphyrin dyes have been developed as promising candidates for DSSCs due to their efficient light-harvesting capability and tunable spectral properties and energetics.[4] Impressively, the DSSC based on porphyrin sensitizer SM315 have reaped a efficiency record of 13.0% without the assistance of any co-sensitizer.[5] However, in view of the limited ruthenium resource and the complicated synthetic procedure for porphyrin dyes, it is desirable to develop metal-free organic dyes[6] for the coming large-scale application of cost-effective DSSCs due to their unique advantages, such as high molar-extinction coefficients,

low synthetic and purification cost, tunable photophysical properties via molecular engineering, and essentially no resource limitation. Most recently, considerable efforts have been made to develop metal-free organic dyes and impressive efficiencies in the range of 10~12% have been achieved.[7] However, most highly efficient DSSCs have been realized with volatile organic liquid electrolytes, which have a drastic effect on the DSSC long-term stability and limit their outdoor applications. To overcome such shortcoming, alternative non-volatile ionic liquid or non-flowing (quasi-)solid-state electrolyte[8] have been utilized in DSSCs and demonstrated greatly improved long-term stability for potential applications in DSSCs. Therefore, concerning the promising outdoor applications, highly efficient and stable DSSCs with non-liquid electrolyte are still required.

Open-circuit voltage (V_{oc}) and short-circuit current (J_{sc}) are two fundamental parameters for the DSSC performance. To improve the value of the latter parameter, it is essential to expand the absorption spectrum of the organic sensitizer meanwhile maintaining suitable energy levels. The simplest way for lowering down the sensitizer band gap is to strengthen the intramolecular charge transfer (ICT) interactions in the organic dye with D-π-A configuration. Recently, we have incorporated auxiliary electron donor (D') and electron acceptor (A'), respectively, into D-π-A featured organic dyes and found

This journal is © The Royal Society of Chemistry 2013

J. Mater. Chem. A, 2014, **2**, 1-11 | **1**

that D-A'-π-A configuration is superior to D-D'-π-A one in bathochromically shifting the sensitizer absorption spectrum, enhancing the light-harvesting efficiency, and improving the photocurrent and device efficiency.[9] Meanwhile, electron-deficient group, such as benzothiadiazole,[10] diketopyrrolopyrrole,[11] and pyrazine derivatives,[12] has been integrated as an auxiliary acceptor (A') to construct novel D-(π)-A'-π-A framework by several groups. The relationship between the chemical structure of the auxiliary acceptor A' and the photophysical and photovoltaic properties of the related sensitizer has been systematically investigated. However, few work has been carried out to optimize the other moieties in the D-(π)-A'-π-A framework.[13] In this contribution, other building blocks, such as the π bridge and the anchoring groups, are adjusted on quinoxaline based organic sensitizer to tune the related photophysical and photovoltaic properties. Ethylenedioxythiophene (EDOT),[14] one of the most popular building blocks in organic semiconductors, is utilized as π-conjugation bridge and two types organic sensitizers with D-A'-π-A (**FNE60** and **FNE61**) and D-π-A'-π-A (**FNE62** and **FNE63**) frameworks have been constructed, as shown in Fig. 1. For comparison, our previously reported sensitizer **FNE46**[12k] is included as reference. It is found that D-π-A'-π-A configuration is superior to D-A'-π-A configuration in expanding the absorption spectrum and enhancing the light-harvesting capability and photocurrent generation. In addition, a much stronger electron withdrawing group, rhodanine-3-acetic acid,[15] is incorporated as an anchoring group instead of the traditional cyanoacrylic acid group. Although significant bathochromic shift can be observed for the absorption maxima of sensitizers **FNE61** and **FNE63**, the related quasi-solid-state DSSCs exhibit less effective electron injection. Consequently, the quasi-solid-state DSSC based on D-π-A'-π-A featured sensitizer **FNE62** with cyanoacrylic acid as anchoring group exhibits a highest power conversion efficiency of 8.2% with good long-term stability after continuous light soaking.
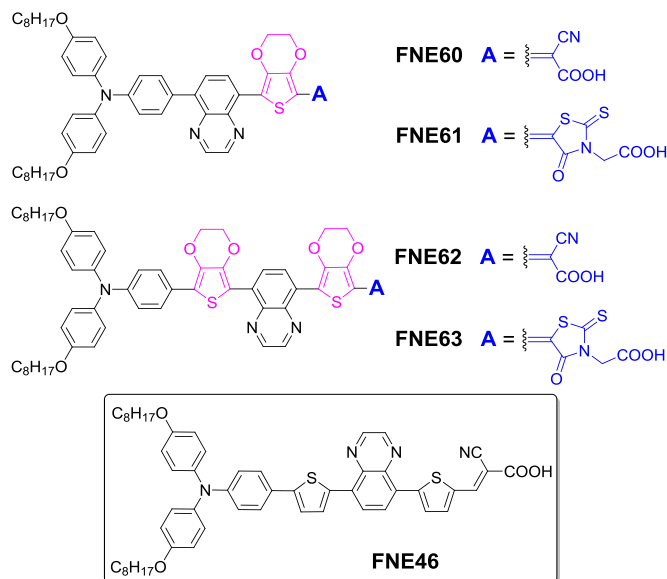
Fig. 1 Chemical structures of sensitizers **FNE60**, **FNE61**, **FNE62**, **FNE63**, and reference **FNE46**.

Experimental Section

Materials and Reagents. Glyoxal (40 wt% solution in H_2O), benzil, 3,4-ethylenedioxythiophene (EDOT), N-bromosuccinimide (NBS), cyanoacetic acid and rhodanine-3-acetic acid were purchased from J&K Chemical Ltd. Purification of organic solvents used in this work was under the standard process. Other chemicals and reagents were used as received from commercial suppliers without further purification. Transparent conductive glass (F-doped SnO_2, FTO, 14 Ω per square, transmittance of 85%, Nippon Sheet Glass Co., Japan) was used as the substrate for the fabrication of DSSC.

Synthesis of 5-bromo-8-(2,3-dihydrothieno[3,4-b][1,4]dioxin-5-yl)quinoxaline (2). A mixture of 5,8-dibromoquinoxaline (**1**)[16] (1.0 g, 3.5 mmol), Pd(PPh₃)₄ (150 mg, 0.13 mmol), tributyl(2,3-dihydrothieno[3,4-b][1,4]dioxin-5-yl)stannane[17] (1.5 g, 3.5 mmol) and N,N-dimethylformamide (DMF) (30 mL) was stirred at 90 ℃ for 15 h under nitrogen atmosphere. After removal of excess solvent, the residue was purified by flash column chromatography (silica gel, dichloromethane (DCM) / petroleum ether (PE) = 1/1). Yellow solid **2** was obtained with a yield of 72% (855 mg). ¹H NMR (400 MHz, CDCl₃, δ ppm): 8.93 (d, 2H, J = 8.3Hz), 8.40 (d, 1H, J = 8.3 Hz), 8.06 (d, 1H, J = 8.3 Hz), 6.57 (s, 1H), 4.40-4.32 (m, 2H), 4.32-4.23 (m, 2H). ¹³C NMR (100 MHz, CDCl₃, δ ppm): 146.3, 145.2, 143.5, 141.6, 133.9, 133.8, 132.7, 129.1, 124.2, 121.2, 112.1, 104.1, 65.2, 64.5.

Synthesis of 7-(8-bromoquinoxalin-5-yl)-2,3-dihydrothieno[3,4-b][1,4]dioxine-5-carbaldehyde (3). A mixture of compound **2** (400 mg, 1.2 mmol) and DMF (134 mg, 1.8 mmol) were dissolved in 30 mL DCM under nireogen atmosphere. Phosphorus oxychloride (0.4 mL, 3.4 mmol) was added dropwise to this solution. The reaction was kept at 80 ℃ for 14 h. After cooling to room temperature, 15 mL saturated sodium acetate aqueous solution was added into the reaction mixture. The mixture was extracted with DCM, and the organic phase was collected and dried over anhydrous sodium sulfate. The solvent was removed with a rotary evaporator and the residue was purified on a silica gel column with DCM/PE (1/1, v/v) as a eluent. Yellow solid **3** was obtained with a yield 90 % (390 mg). ¹H NMR (400 MHz, CDCl₃, δ ppm): 10.03 (s, 1H), 9.01 (d, 2H, J = 8.4 Hz), 8.54 (d, 1H, J = 8.4 Hz), 8.15 (d, 1H, J = 8.4 Hz), 4.47 (s, 4H). ¹³C NMR (100 MHz, CDCl₃, δ ppm): 181.0, 149.2, 147.4, 144.2, 142.4, 135.1, 133.5, 132.9, 130.5, 127.2, 120.5, 110.4, 103.5, 64.6, 64.3.

Synthesis of 7-(8-(4-(bis(4-(octyloxy)phenyl)amino)phenyl)quinoxalin-5-yl)-2,3-dihydrothieno[3,4-b][1,4]dioxine-5-carbaldehyde (4). A mixture of compound **3** (200 mg, 0.32 mmol), N,N-bis[4-(octyloxy)phenyl]-4-(4,4,5,5-tetramethyl-1,3,2-dioxaborolan-2-yl)aniline[12k] (120 mg, 0.32 mmol), Pd(PPh₃)₄ (30 mg, 0.02 mmol) and K₂CO₃ (2.76 g, 0.02 mol) in a mixed solution of toluene (30 mL) and water (5 mL)was stirred and heated at 90 ℃ for 24 h under nitrogen atmosphere. When the reaction was completed, the mixture was extracted with DCM for three times. The combined organic solution was washed with brine and dried by anhydrous sodium sulfate. The solvent was removed with a rotary evaporator and the residue was purified on a silica gel column with DCM/PE (2/1, v/v) as eluent. Dark red solid **4** was obtained with a yield 79% (200mg). ¹H NMR (400 MHz, CDCl₃, δ ppm): 10.02 (s, 1H), 8.92 (d, 2H, J = 8.0 Hz), 8.66 (d, 1H, J = 8.0 Hz), 7.83 (d, 1H, J = 7.9 Hz), 7.55 (d, 2H, J = 8.5 Hz), 7.14 (d, 4H, J = 8.8 Hz), 7.02 (d, 2H, J = 8.6 Hz), 6.85 (d, 4H, J = 8.8 Hz), 4.46 (s, 4H), 3.94 (t, 4H, J = 6.5 Hz), 1.85-1.72 (m, 4H), 1.45 (d, 4H, J = 7.8 Hz), 1.29 (t, 16H, J = 6.6 Hz), 0.89 (t, 6H, J = 6.5 Hz). ¹³C NMR (100 MHz, CDCl₃,

2 | *J. Mater. Chem. A*, 2014, **2**, 1-11

This journal is © The Royal Society of Chemistry 2014

δ ppm): 183.4, 154.9, 153.2, 149.1, 148.6, 148.5, 144.9, 144.3, 144.2, 140.0, 139.9, 136.7, 136.1, 135.2, 129.1, 128.8, 127.6, 126.4, 125.7, 120.8, 120.6, 116.1, 70.6, 68.4, 66.1, 33.2, 29.6, 29.4, 28.9, 26.0, 23.1, 14.4.

Synthesis of 7-(8-(7-(4-(bis(4-(octyloxy)phenyl)amino)phenyl)-2,3-dihydrothieno[3,4-b][1,4]dioxine-5-yl)quinoxalin-5-yl)-2,3-dihydrothieno[3,4-b][1,4]dioxine-5-carbaldehyde (5). A mixture of compound **3** (147 mg, 0.39 mmol), Pd(PPh$_3$)$_4$ (100 mg, 0.09 mmol), N,N-bis[4-(octyloxy)phenyl]-4-(7-(tributylstannyl)-2,3-dihydrothieno[3,4-b][1,4]dioxin-5-yl)aniline[9] (363 mg, 0.39 mmol) and 30 mL DMF was stirred at 90 °C for 15 h under nitrogen atmosphere. After removal of excess solvent, the residue was purified by flash column chromatography with DCM/PE (2/1, v/v) as eluent. Black solid **5** was obtained with a yield of 65% (238 mg). ^{1}H NMR (400 MHz, CDCl$_3$, δ ppm): 10.01 (s, 1H), 8.95 (d, 2H, J = 6.7 Hz), 8.69 (s, 2H), 7.65 (d, 2H, J = 8.8 Hz), 7.06 (d, 4H, J = 8.8 Hz), 6.95 (d, 2H, J = 8.9 Hz), 6.82 (d, 4H, J = 8.9 Hz), 4.46 (s, 8H), 3.93 (t, 4H, J = 6.5 Hz), 1.85-1.72 (m, 4H), 1.45 (d, 4H, J = 7.8 Hz), 1.40-1.21 (m, 16H), 0.90 (m, 6H). ^{13}C NMR (100 MHz, CDCl$_3$, δ ppm): 182.2, 154.3, 154.2, 148.8, 148.5, 148.2, 145.2, 144.1, 143.8, 140.2, 140.1, 139.8, 136.1, 136.0, 134.3, 129.2, 128.8, 127.2, 127.0, 126.7, 125.9, 121.0, 120.4, 115.6, 69.7, 66.2, 65.3, 32.1, 29.8, 29.6, 29.5, 26.3, 22.9, 14.6.

Synthesis of sensitizer FNE60. Under a nitrogen atmosphere, a mixture of compound **4** (150 mg, 0.19 mmol) and cyanoacetic acid (39 mg, 0.45 mol) in acetonitrile (15 mL) was refluxed in the presence of piperidine (0.1 mL) for 15 h. After cooling to room temperature, poured into water and extracted with DCM, the combined organic solution was washed with water and sodium chloride solution and dried over anhydrous sodium sulfate. After removal of the solvent, the residue was purified by flash column chromatography (silica gel, DCM/MeOH = 10/1). Black solid, yield 75% (122 mg). ^{1}H NMR (400 MHz, DMSO-d_6, δ ppm): 9.01-8.99 (m, 2H), 8.69 (d, 1H, J = 7.9 Hz), 8.22 (s, 1H), 7.92 (d, 1H, J = 7.6 Hz), 7.56 (d, 2H, J = 8.0 Hz), 7.07 (d, 4H, J = 8.6 Hz), 6.93 (d, 4H, J = 8.6 Hz), 6.84 (d, 2H, J = 8.3 Hz), 4.51 (s, 4H), 3.93 (t, 4H, J = 5.9 Hz), 1.69 (d, 4H, J = 6.7 Hz), 1.40 (m, 4H), 1.35-1.30 (m, 16H), 0.87-0.84 (m, 6H). ^{13}C NMR (100 MHz, DMSO-d_6, δ ppm): 159.1, 153.9, 153.0, 149.7, 149.6, 148.4, 144.8, 144.5, 144.2, 140.1, 139.5, 136.9, 136.5, 135.3, 129.2, 128.9, 127.6, 126.5, 125.8, 120.9, 120.4, 117.7, 70.7, 68.6, 66.1, 65.3, 32.5, 30.0, 29.9, 26.7, 23.2, 14.1. HRMS (ESI, m/z): [M+H]$^+$ calcd for C$_{52}$H$_{57}$N$_4$O$_6$S, 865.3999; found, 865.3985.

Synthesis of sensitizer FNE61. Under a nitrogen atmosphere, a mixture of compound **4** (150 mg, 0.19 mmol) and rhodanine-3-acetic acid (57 mg, 0.30 mol) in acetonitrile (15 mL) was refluxed in the presence of piperidine (0.1 mL) for 15 h. After cooling to room temperature, poured into water and extracted with DCM, the combined organic solution was washed with water and sodium chloride solution and dried over anhydrous sodium sulfate. After removal of the solvent, the residue was purified by flash column chromatography (silica gel, DCM/MeOH = 10/1). Black solid, yield 43% (79 mg). ^{1}H NMR (400 MHz, DMSO-d_6, δ ppm): 9.07-9.00 (m, 2H), 8.72 (d, 1H, J = 7.8 Hz), 8.01 (d, 1H, J = 7.8 Hz), 7.93(s, 1H), 7.60 (d, 2H, J = 8.2 Hz), 7.14 (d, 4H, J = 8.5 Hz), 7.01 (d, 4H, J = 8.5 Hz), 6.92 (d, 2H, J = 8.3 Hz), 4.51-4.45 (m, 6H), 4.02 (t, 4H, J = 5.9 Hz), 1.67 (d, 4H, J = 6.9 Hz), 1.44 (m, 4H), 1.34-1.30 (m, 16H), 0.87-0.84 (m, 6H).^{13}C NMR (100 MHz, DMSO-d_6, δ ppm): 193.7, 166.2, 164.5, 154.2, 153.9, 153.0, 149.3, 148.5, 148.1, 146.1, 144.3, 140.2 139.9, 136.7, 136.6, 135.7, 130.1, 128.8,

128.4, 126.1, 125.9, 120.6, 120.4, 118.9, 70.1, 68.9, 67.3, 64.2, 61.3, 56.0, 47.2, 33.5, 30.9, 29.6, 26.3, 23.1, 13.7. HRMS (ESI, m/z): [M+H]$^+$ calcd for C$_{54}$H$_{59}$N$_4$O$_7$S$_3$, 971.3546; found 971.3540.

Synthesis of sensitizer FNE62. Compound **FNE62** was synthesized from compound **5** similarly as described as that for compound **FNE60**. Black solid yield 60% (84 mg). ^{1}H NMR (400 MHz, DMSO-d_6, δ ppm): 9.13-9.09 (m, 2H), 8.70 (d, 1H, J = 7.6 Hz), 8.03 (d, 1H, J = 7.6 Hz), 7.99(s, 1H), 7.60 (d, 2H, J = 8.1 Hz), 7.11 (d, 4H, J = 8.6 Hz), 6.98 (d, 4H, J = 8.6 Hz), 6.87 (d, 2H, J = 8.2 Hz), 4.50-4.45 (m, 8H), 3.90 (t, 4H, J = 6.0 Hz), 1.58-1.56 (m, 4H), 1.43-1.40 (m, 4H), 1.36-1.33 (m, 16H), 0.94-0.94 (m, 6H). ^{13}C NMR (100 MHz, DMSO-d_6, δ ppm): 157.8, 150.1, 149.0, 145.4, 145.3, 145.0, 144.3, 142.1, 140.8, 138.4, 138.2, 137.1, 135.2, 131.1, 129.9, 129.1, 128.90, 128.3, 128.2, 128.1, 127.4, 127.1, 122.0, 121.6, 117.3, 68.32, 65.1, 33.4, 31.2, 30.1, 29.9, 27.6, 23.2, 14.2. HRMS (ESI, m/z): [M+H]$^+$ calcd for C$_{58}$H$_{60}$N$_4$O$_8$S$_2$, 1005.3931; found, 1005.3916.

Synthesis of sensitizer FNE63. Compound **FNE63** was synthesized from compound **5** similarly as described as that for compound **FNE61**. Black solid, yield 42% (62 mg). ^{1}H NMR (400 MHz, DMSO-d_6, δ ppm): 9.04-8.98 (m, 2H), 8.69 (d, 1H, J = 7.9 Hz), 8.00 (d, 1H, J = 7.9 Hz), 7.98 (s, 1H), 7.62 (d, 2H, J = 8.0 Hz), 7.20 (d, 4H, J = 8.1 Hz), 7.11 (d, 4H, J = 8.2 Hz), 6.91 (d, 2H, J = 8.2 Hz), 4.50-4.43 (m, 10H), 4.01 (t, 4H, J = 6.0 Hz), 1.63 (d, 4H, J = 7.0 Hz), 1.42 (m, 4H), 1.34-1.29 (m, 16H), 0.90-0.86 (m, 6H). ^{13}C NMR (100 MHz, DMSO-d_6, δ ppm): 196.1, 165.1, 164.3, 154.6, 154.0, 153.5, 149.7, 149.3, 148.3, 145.6, 145.1, 142.3 140.1, 138.1, 137.8, 136.5, 131.4, 129.6, 129.0, 128.6, 127.1, 121.3, 121.0, 120.1, 72.6, 70.1, 68.9, 65.6, 64.9, 62.0, 58.3, 46.7, 32.1, 29.9, 29.1, 25.9, 24.0, 14.0. HRMS (ESI, m/z): [M+H]$^+$ calcd for C$_{60}$H$_{63}$N$_4$O$_9$S$_4$, 1111.3478; found 1111.3483.

Characterizations. ^{1}H NMR (400 MHz) and ^{13}C NMR (100 MHz) spectra were measured on a Varian Mercury Plus-400 spectrometer. The splitting patterns are designated as follows: s (singlet); d (doublet); t (triplet); m (multiplet). UV–vis absorption spectra of the dyes were measured in toluene solutions and on TiO$_2$ films with a Shimadzu UV–2550PC spectrophotometer. The film thickness was measured by a surface profiler (Veeco Dektak 150). Cyclic voltammetry measurements were performed with a CHI604D electrochemical workstation using a conventional three-electrode electrochemical cell in a solution of tetrabutylammonium hexafluorophosphate (0.1 M) in water-free acetonitrile at a scan rate of 50 mV s^{-1} at room temperature under argon. Dye-adsorbed TiO$_2$ film (0.25 cm^2) on conductive FTO glass was used as the working electrode, a Pt wire as the counter electrode, and an Ag/Ag$^+$ electrode as the reference electrode. The potential of the reference electrode was calibrated by ferrocene, and all potentials mentioned in this work are against the normal hydrogen electrode (NHE).

DSSC Fabrication and Photovoltaic Measurements. The working electrode was composed of a TiO$_2$ nanoparticle (20 nm) film (active area 0.25 cm^2) direct contact with the FTO substrate. The films were sintered at 500 °C for 2 h to achieve good necking of neighboring TiO$_2$ particles. The sintered films were then treated with 0.05 M TiCl$_4$ aqueous solution at 70 °C for 30 min followed by calcinations at 450 °C for 30 min. When TiO$_2$ electrodes were cooled down at around 120 °C, the electrodes were dipped in dye solutions (0.3 mM in chloroform/ethanol, 7/3, v/v) with deoxycholic acid as coadsorbate for 24 h at room temperature for complete dye adsorption. The counter electrode was prepared by coating with a drop of H$_2$PtCl$_6$ solution on an FTO plate and heating at 400 °C for

This journal is © The Royal Society of Chemistry 2014

J. Mater. Chem. A, 2014, **2**, 1-11 | **3**

30 min. The dye-adsorbed TiO$_2$ electrode and Pt-counter electrode were separated by a hot-melt Surlyn film (30 μm) and sealed together by pressing them under heat. Quasi-solid-state gel electrolyte was prepared by mixing 5% (wt%) poly(vinylidenefluoride-co-hexafluoropropylene) in a redox solution containing 0.1 M LiI, 0.1 M I$_2$ 0.6 M 1,2-dimethyl-3-*n*-propylimidazolium iodide (DMPImI), and 4-*tert*-butylpyridine (TBP) in 3-methoxypropionitrile (MPN) under heating until all solids were dissolved. After introducing the hot gel solution into the internal space of the cell from the two holes predrilled on the back of the counter electrode, a uniform motionless polymer gel layer was formed between the working and the counter electrodes, and then the holes were sealed with a Surlyn film covered with a thin glass slide under heat. The working performance of DSSCs was tested by recording the current density-voltage (*J-V*) curves with a Keithley 2400 source meter (Oriel) under the illumination of simulated AM1.5G solar light coming from a solar simulator (Sol3A equipped

with a 450 W Xe lamp and an AM1.5G filter). The incident light intensity was calibrated using a standard Si solar cell (Newport 91150). Action spectra of the incident monochromatic photon-to-electron conversion efficiency (IPCE) for the solar cells were obtained with an Oriel-74125 system (Oriel). The intensity of monochromatic light was measured with a Si detector (Oriel-71640).The electron lifetimes were measured with intensity modulated photovoltage spectroscopy (IMVS), and charge densities at open-circuit were measured using charge extraction technique. IMVS analysis and charge extraction were carried out on an electrochemical workstation (Zahner XPOT, Germany), which includes a white light emitting diode and corresponding control system. The intensity modulated spectra were measured at room temperature with light intensity ranging from 20 to 120 W m^{-2}, in modulation frequency ranging from 0.1 Hz to 10 kHz, and with modulation amplitude less than 5% of the light intensity.
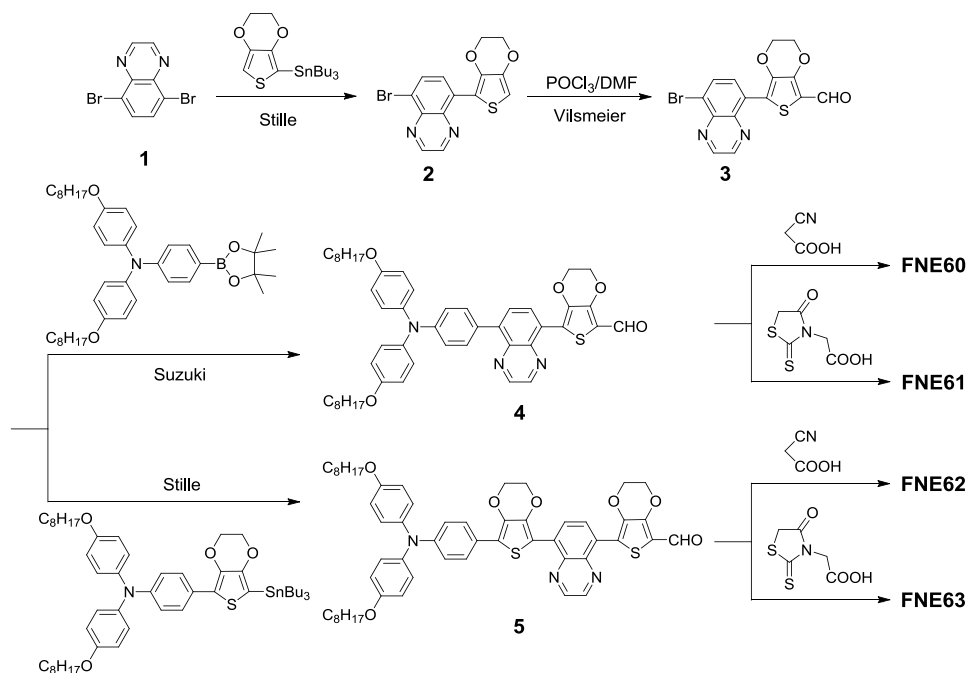
Scheme 1 Synthetic routes for sensitizers **FNE60**, **FNE61**, **FNE62**, and **FNE63**.

Results and Discussion

Synthesis of Sensitizers

As depicted in Scheme 1, the syntheses for all the sensitizers started from 5,8-dibromoquinoxaline (**1**),[16] which was then converted to 5-bromo-8-(2,3-dihydrothieno[3,4-*b*][1,4]dioxin-5-yl)quinoxaline (**2**) via an asymmetrical Stille coupling[18] with tributyl(2,3-dihydrothieno[3,4-*b*][1,4]dioxin-5-yl)stannane.[17] After refluxing with a Vilsmeier reagent,[19] the corresponding monoaldehyde-substituted derivative **3** was provided. A further Suzuki coupling[20] with *N,N*-bis(4-(octyloxy)phenyl)-4-(4,4,5,5-tetramethyl-1,3,2-dioxaborolan-2-yl)aniline[1k] afforded the precursor **4**. Herein, octyloxy substituted triarylamine was incorporated instead of traditional triphenylamine due to the following consideration. Firstly, the two octyloxy substituents can ensure sufficient solubility of the target sensitizers in common organic solvents. Secondly, alkoxyl functionalized triarylamine is more electron-rich than triphenylamine, which

may enlarge the ICT interactions and thus reduce the band gap. Finally, the introduced alkoxyl chains can effectively weaken the intermolecular aggregation and charge recombination during the DSSC operation, which is beneficial to reducing the current and voltage losses. However, it should be noted that for the synthesis of precursor **5**, a two-step coupling with EDOT and further with *N,N*-bis(4-(octyloxy)phenyl)aniline on compound **3** was not straightforward due to the difficult functionalization of EDOT derivative. Therefore, precursor **5** was alternatively obtained via a direct Stille coupling between the key intermediate compound **3** and *N,N*-bis(4-(octyloxy)phenyl)-4-(7-(tributylstannyl)-2,3-dihydrothieno[3,4-*b*][1,4]dioxin-5-yl)aniline.[9] In the last step, the obtained two precursors were converted to the four target sensitizers **FNE60**, **FNE61**, **FNE62**, and **FNE63**, respectively, by Knoevenagel condensation[21] with cyanoacetic acid or rhodanine-3-acetic acid in the presence of piperidine. All the target dye sensitizers were characterized by ^{1}H NMR, ^{13}C NMR spectroscopy, and mass spectroscopy, and were found to be consistent with the proposed structures. The obtained dyes are black in solid state,

4 | *J. Mater. Chem. A*, 2014, **2**, 1-11

This journal is © The Royal Society of Chemistry 2014
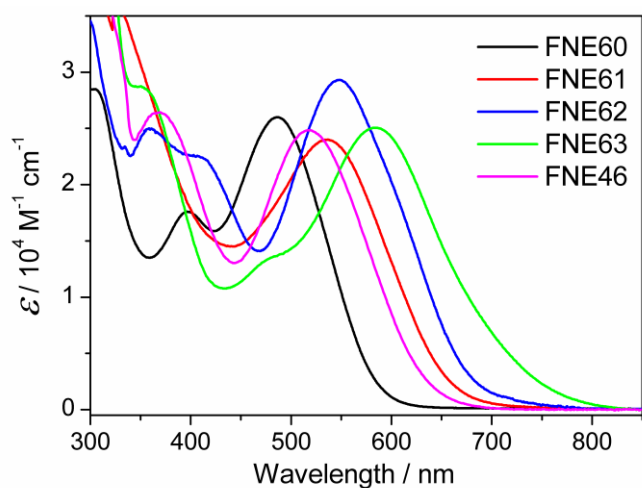
Fig. 2 UV-vis absorption spectra of the organic sensitizers in toluene solutions.
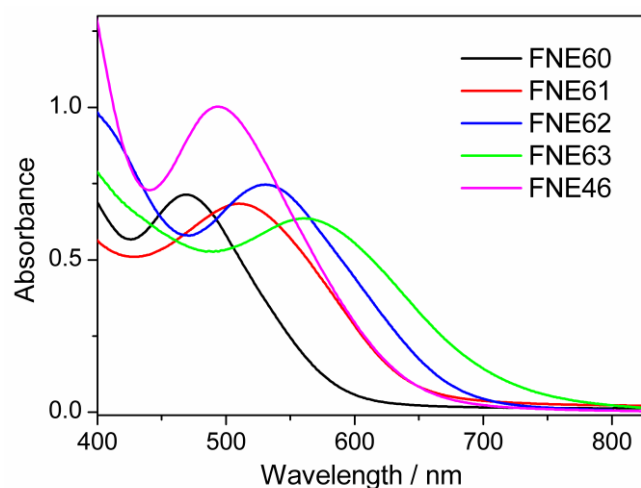
Fig. 3 UV-vis absorption spectra of the organic sensitizers on 3 μm thick TiO$_2$ films.

Table 1. UV-vis absorption and electrochemical properties of sensitizers **FNE60**, **FNE61**, **FNE62**, and **FNE63**.

| Dye | Absorption | | | HOMO^b | E_g | LUMO^b |
	λ_{max}^a nm	ε^a M^{-1} cm^{-1}	λ_{max} on TiO$_2$ nm	V	eV	V
FNE60	486	2.6×10^4	469	0.94	2.09	-1.15
FNE61	537	2.4×10^4	511	0.90	1.88	-0.98
FNE62	548	2.9×10^4	531	0.78	1.82	-1.04
FNE63	584	2.5×10^4	562	0.75	1.67	-0.92

^{a} Absorption peaks (λ_{max}) and molar extinction coefficients (ε) were measured in toluene solutions (~10^{-5} M). ^{b} The potentials (vs. NHE) were calibrated with ferrocene.

and can be dissolved in common organic solvents, such as dichloromethane, THF and toluene.

Photophysical Properties

The UV-vis absorption spectra (Fig. 2) of sensitizers **FNE60**, **FNE61**, **FNE62**, and **FNE63** in toluene solutions were measured at a concentration of ca. 10^{-5} M, and the corresponding photophysical data are listed in Table 1. It can be found that all the sensitizers exhibit two distinct absorption bands, which is similar to that for reference sensitizer **FNE46**.[12k] The absorption band in the visible region corresponds to the charge transfer between the electron donating unit and the electron withdrawing group, and the other one in the ultraviolet region can be assigned to the π–π* electron transition of the conjugated backbone. As shown in Fig. 2, sensitizer **FNE60** exhibits the maximum absorption wavelength at 486 nm in toluene solution. Upon replacing the cyanoacetic acid in **FNE60** with a stronger electron acceptor in **FNE61**, i.e., rhodanine-3-acetic acid, a dramatic bathochromic shift of 51 nm can be observed for the maximum absorption wavelength, which is obviously stemmed from the strengthened ICT interactions after introduction of rhodanine-3-acetic acid. When an auxiliary **EDOT** unit was inserted between the triarylamine and quinoxaline units in **FNE60**, sensitizer **FNE62** displays the absorption maximum wavelength at 548 nm with a more significant bathochromic shift of 62 nm and increased molar extinction coefficient in comparison to that for sensitizer **FNE60**. It should be noted that a bathochromic shift of 23 nm can be observed as compared with reference sensitizer **FNE46**,[12k] which exhibits the absorption maximum at 525 nm in chloroform solution. Such a remarkable bathochromic shift is obviously due to the more electron

donating capability of **EDOT** spacer as compared with thiophene one. Moreover, when the cyanoacrylic acid unit in sensitizer **FNE62** is replaced by rhodanine-3-acetic acid unit, sensitizer **FNE63** exhibited the maximum absorption wavelength at 583 nm with a bathochromic shift of 36 nm in comparison to that for sensitizer **FNE62**, which is similar to those for sensitizers **FNE60** and **FNE61**. These results suggest that not only stronger electron donating spacer but also stronger electron acceptor contribute to reducing the sensitizer band gap and improving light-harvesting properties. Moreover, in comparison to sensitizers **FNE60** and **FNE61** with D-A'-π-A configuration, sensitizers **FNE62** and **FNE63** with D-π-A'-π-A configuration exhibit bathochromically shifted absorption maxima by 62 and 47 nm, respectively, which indicates that D-π-A'-π-A framework is superior to D-A'-π-A configuration in expanding the absorption spectrum and enhancing the light-harvesting capability.

The UV-vis absorption spectra for the dye-loaded TiO$_2$ films are shown in Fig. 3. Sensitizers **FNE60**, **FNE61**, **FNE62**, and **FNE63** demonstrate the maximum absorption wavelength at 469, 511, 531, and 562 nm, respectively, which displays the same trend as those in toluene solutions. A slight hypsochromic shift of 17, 26, 17, and 22 nm, respectively, can be found for the absorption maxima of dye-loaded TiO$_2$ films in comparison to those for the dye solutions. Since no obvious shift can be observed for the maximum absorption wavelength of the sensitizers in different concentration solutions, such a hypsochromic shift for the absorption maxima is mainly due to the deprotonation effect after the dye molecules are anchored on nanocrystalline TiO$_2$ films.[12j,12k,22] However, the hypsochromic shift is much smaller than those for D-π-A featured organic dyes,[23] which

This journal is © The Royal Society of Chemistry 2014

J. Mater. Chem. A, 2014, 2, 1-11 | 5
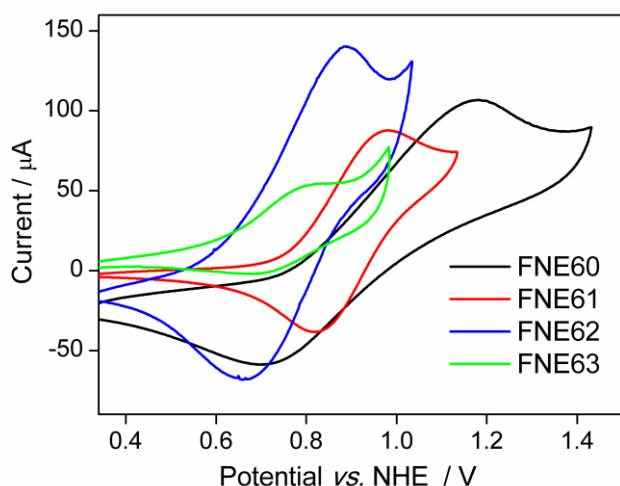
Fig. 4 Cyclic voltammograms of the dye-loaded TiO$_2$ films (0.25 cm^2).

is obviously due to the weakened deprotonation effect caused by the auxilary quinoxaline acceptor. When the dye molecules are adsorbed on TiO$_2$ surface, although the anchoring acid group is deprotonated, the charge transfer from the electron donor to the auxilary quinoxaline moiety is not affected significantly and therefore only slight hypsochromic shift can be observed for organic dyes with both D-A'-π-A and D-π-A'-π-A configuration.

Electrochemical Properties.

To investigate the possibility of the photo-generated electron injection and the sensitizer regeneration, cyclic voltammetry was performed in a conventional three-electrode electrochemical cell with dye-loaded TiO$_2$ film as the working electrode. Fig. 4 displays the cyclic voltammograms of the four sensitizers and it can be found that all the dyes display reversible oxidative curves, which correspond to the removal of electrons at the triarylamine moieties to form the stable radical cations. As shown in Fig. 4, sensitizer **FNE60** displays a reversible anodic redox couple at half-wave potential ($E_{1/2}$) of 0.94 V versus normal hydrogen electrode (NHE), which corresponds to the highest occupied molecular orbital (HOMO) level. Upon the replacing of the cyanoacrylic acid in **FNE60** by a rhodanine-3-acetic acid, negatively shifted oxidation potential can be observed for sensitizer **FNE61** (0.90). Moreover, when an EDOT unit is incorporated into the conjugation backbone of sensitizer **FNE60**, sensitizer **FNE62** displays negatively shifted oxidation potential at $E_{1/2}$ = 0.78 V. Furthermore, replacing the cyanoacrylic acid in **FNE62** by a rhodanine-3-acetic acid, sensitizer **FNE63** exhibits further negatively shifted oxidation potential at $E_{1/2}$ = 0.75 V. It should be noted that both the EDOT unit and the rhodanine-3-acetic acid group can lift up the HOMO levels of the organic dyes. The lift contribution from the EDOT unit is higher than that from the rhodanine-3-acetic acid group. This can be attributed to the more delocalized HOMO after incorporation of EDOT unit close to the triarylamine moiety. The HOMO values for all the sensitizers are much more positive than the redox potential for I$^-$/I$_3^-$ redox couples (~0.4 V), indicating that the reduction of the oxidized dyes with I-ions is thermodynamically feasible.[24] Then the LUMO energy level was estimated from equation (1),[25]

$$\text{LUMO} = \text{HOMO} - \Delta E \qquad (1)$$

where ΔE is the energy gap between the HOMO and LUMO levels and derived from the wavelength at 10% maximum absorption

intensity for the dye-loaded TiO$_2$ film.[26] Correspondingly, the LUMO levels for sensitizers **FNE60**, **FNE61**, **FNE62**, and **FNE63**, are calculated to be -1.15, -0.98, -1.04 and -0.92 V, respectively. In comparison to the LUMO levels of **FNE60** and **FNE62**, the positively shifted LUMO levels of **FNE61** and **FNE63**, respectively, are obviously due to the introduction of a much stronger electron acceptor, rhodanine-3-acetic acid, instead of cyanoacrylic acid unit. The LUMO values for all the sensitizers suggest enough driving force of the electron injection from their excited states to the conduction band of TiO$_2$ semiconductors.[24]

Theoretical Approach
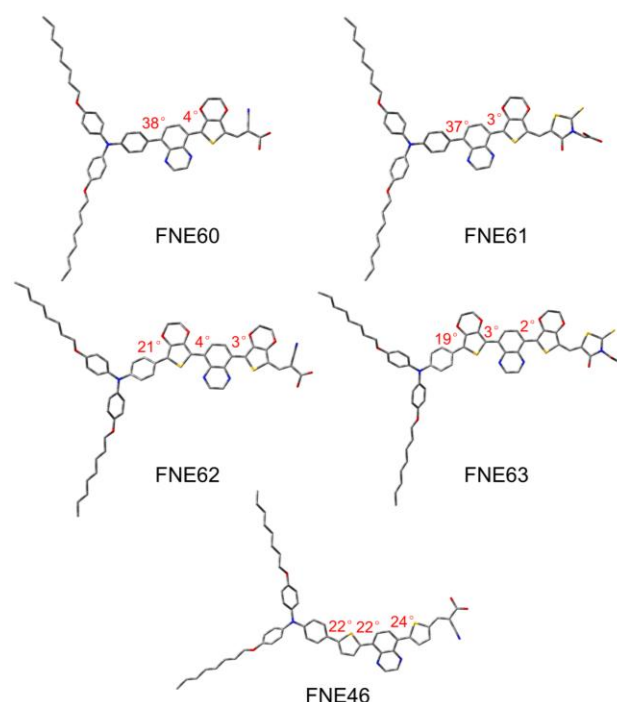
Fig. 5 Optimized ground state geometry and related dihedral angles for the organic sensitizers.

To have deep insight into the ground state geometry and electronic properties of the four organic dyes, density functional calculations were carried out with the Gaussian 03 program using B3LYP method and 6-31G* basis set.[27] As shown in the optimized conformation (Fig. 5), the dihedral angles between the quinoxaline unit and the neighboured benzene ring in sensitizers **FNE60** and **FNE61** are calculated to be 38° and 37°, respectively, which are generalized observation for dihedral angles between two benzene rings. While the dihedral angles between the quinoxaline unit and another neighboured EDOT unit are calculated to be 4° and 3°, respectively. The values are much smaller than the dihedral angles (22° and 24°) between the quinoxaline unit and thiophene ring in sensitizer **FNE46**, which is probably due to the formation of hydrogen bond between the O atom in the EDOT unit and the H atom in the quinoxaline unit. However, when an auxilary EDOT unit is incorporated between the triarylamine and quinoxaline, the dihedral angles between the benzene ring in the triarylamine moiety and the inserted EDOT unit in sensitizers **FNE62** and FNE63 decreases to 21° and 19°, respectively. While the dihedral angles between the quinoxaline unit and the two neighboured EDOT groups are calculated to be 2-4°. It should be noted that when an auxaliary EDOT unit is

6 | *J. Mater. Chem. A*, 2014, **2**, 1-11

This journal is © The Royal Society of Chemistry 2014

inserted between the triarylamine and quinoxaline in sensitizers **FNE60** and **FNE61** with D-A'-π-A configuration, a less twisted molecular structure can be observed for both sensitizers **FNE62** and **FNE63** with D-π-A'-π-A configuration. Therefore, in addition to the π-conjugation elongation upon the incorporation of EDOT unit, a more delocalized π-conjugation can be realized in the D-π-A'-π-A featured organic sensitizers, which therefore results in the extended effective π-conjugation length and is consistent with significant difference in the absorption spectra in Fig. 2.

Fig. 6 shows the calculated frontier molecular orbitals of the found sensitizers. It can be clearly found that for all the sensitizers, the HOMOs mainly delocalize on the triarylamine moiety with extension to the bridged quinoxaline and EDOT moieties, while the LUMOs mainly delocalize over the two acceptors and the EDOT linker. The overlap of the HOMOs

and LUMOs facilitates the charge transfer from the electron-donating center to the electron-withdrawing center. For sensitizers **FNE60** and **FNE62** with cyanoacrylic acid as anchoring groups, the LUMOs delocalize on the anchoring carboxylic acid moieties. Thus, upon excitation by the sunlight, the excited electrons can easily transfer from the triarylamine center to the carboxylic acid group and further into TiO_2. However, for sensitizers **FNE61** and **FNE63** with rhodanine-3-acetic acid as anchoring groups, the LUMOs delocalize on the rhodanine sulfur atom instead of carboxylic acid moiety, which is probably due to the fact that the methylene group disrupts the π* conjugation between rhodanine and the carboxylic acid.[28] Consequently, the excited electrons may not be effectively injected into the TiO_2 electrode via the rhodanine-3-acetic acid group.
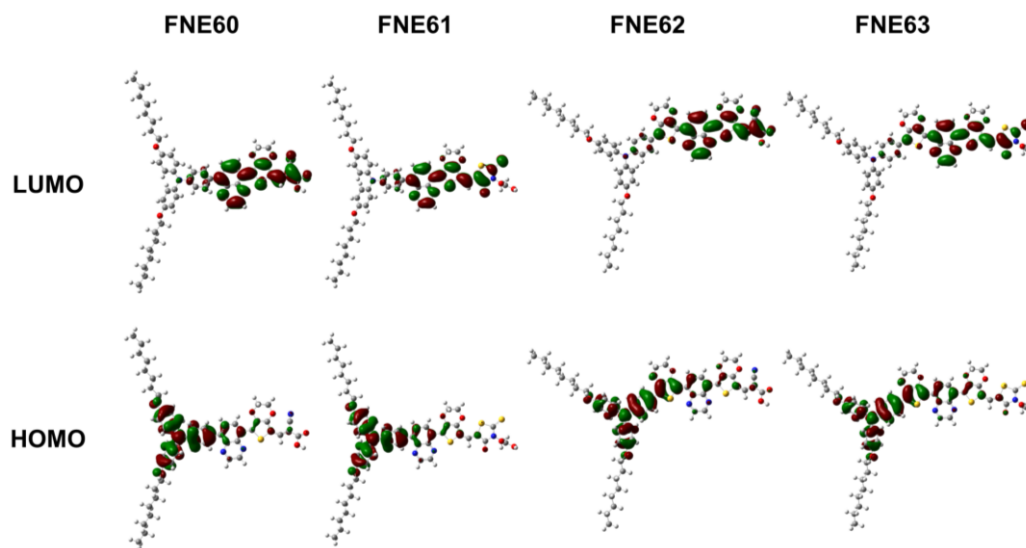
Fig. 6 Calculated frontier molecular orbitals of the four sensitizers.

Table 2 Photovoltaic performance for the quasi-solid-state DSSC based on **FNE62** loaded on TiO_2 films with different thickness.

Thickness μm	V_{oc} mV	J_{sc} mA cm⁻²	FF %	η %
6	705	14.53	68	6.9
10	694	16.34	68	7.7
15	682	17.59	68	8.2
20	675	16.69	67	7.5

Table 3 Photovoltaic performance for **FNE62** based quasi-solid-state DSSC with different concentration of TBP in the electrolyte or DCA in the dye bath.

C_{DCA} mM	C_{TBP} M	V_{oc} mV	J_{sc} mA cm⁻²	FF %	η %
	0.0	654	16.88	69	7.6
10	0.1	682	17.59	68	8.2
	0.2	691	14.31	68	6.7
0		664	15.46	69	7.1
10	0.1	682	17.59	68	8.2
20		633	13.55	64	5.5

Solar Cell Performance

Quasi-solid-state DSSCs based on the four sensitizers were fabricated with a polymer gel electrolyte containing 5% PVDF-HFP (w/w) in MPN. To achieve the best DSSC performance, the thickness of the TiO_2 films, the content of *tert*-butylpyridine (TBP) in the electrolyte and deoxycholic acid (DCA) in the dye bath were optimized for **FNE62** based quasi-solid-state DSSC since it provided the best performance in our initial measurement. Table 2 summarizes the detailed photovoltaic parameters of the quasi-solid-state DSSC (C_{TBP} = 0.1 M, C_{DCA} = 10 mM) based on sensitizer **FNE62** loaded on mesoscopic TiO_2 films with different thickness. It can be found that with the TiO_2 film thickness increasing, the J_{sc} value increases gradually and peaked at 15 μm owning to the enhanced surface area which adsorbs more sensitizers, harvests more sunlight, and provides higher photo-generated current.[29] The J_{sc} value slightly decreases to 16.69 mA cm⁻² on 20 μm TiO_2 film, which is due to the slower electron diffusion and consequently lower electron collection efficiency.[29] However, on the other hand, the V_{oc} value decreases with increasing thickness due to the augmentation of the surface area providing additional charge recombination sites and enhancing the dark current.[29]

To further investigate the relationship between the additive concentration and the quasi-solid-state DSSC performance, the

This journal is © The Royal Society of Chemistry 2014

J. Mater. Chem. A, 2014, **2**, 1-11 | **7**

content of additive TBP in the electrolyte was also optimized (Table 3). When the concentration of TBP increases from 0 to 0.2 M, the V_{oc} value increases slightly from 654 to 691 mV, which is consistent with the reported phenomenon[30] and mainly attributed to the negative shift of conduction band of TiO_2 caused by the adsorption of TBP on TiO_2 surface. On the other hand, J_{sc} value increases from 16.88 to 17.59 mA cm^{-2} upon 0.1 M TBP is added, probably owning to the reduced charge recombination rate, and then decreases to 14.31 mA cm^{-2} at 0.2 M TBP due to the reduced the driving force for the electron injection from the excited dye molecule to the conduction band of TiO_2 semiconductor.

DCA is often utilized as a coadsorbate in the dye bath to suppress the dye aggregation, retard the charge recombination, and improve the DSSC performance. Therefore, the effect of DCA content on the quasi-solid-state DSSC performance was investigated (Table 3). Upon coadsorption of DCA (10 mM), although the the dye-loading amount of **FNE62** decreases from 1.42×10^{-8} mol cm^{-2} μm^{-1} (0 mM DCA) to 0.96×10^{-8} mol cm^{-2} μm^{-1} (10 mM DCA), both the V_{oc} and J_{sc} values significantly increase for **FNE62** based quasi-solid-state DSSC. This is obviously stemmed from the coadsorption of additive DCA, which reduces the charge recombination rate in the DSSCs. However, with further increasing of DCA content, both the V_{oc} and J_{sc} values dramatically decrease probably due to the lower dye adsorbed amount which further reduces to 0.62×10^{-8} mol cm^{-2} μm^{-1}.
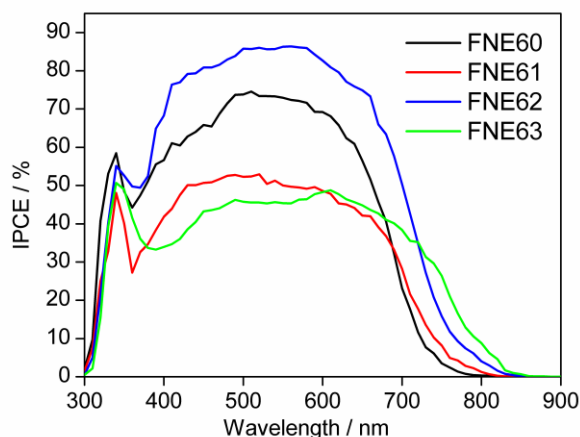
Fig. 7 IPCE spectra for the quasi-solid-state DSSCs.
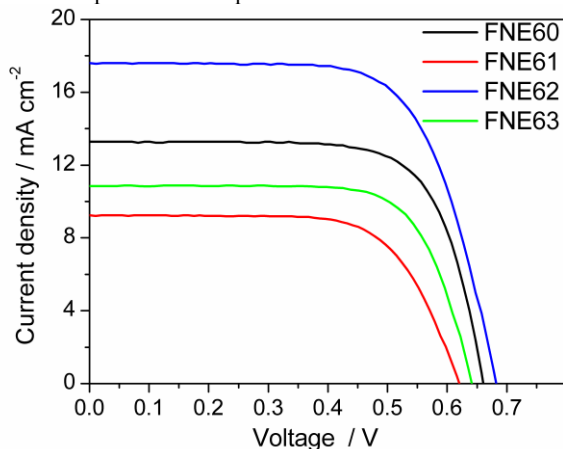
Fig. 8 *J – V* curves for the quasi-solid-state DSSCs.

Therefore, the quasi-solid-state DSSCs based on sensitizers **FNE60-FNE63** were fabricated on 15 μm thick photoanode with 0.1 M TBP in the electrolyte and 10 mM DCA in the dye bath as coadsorbate. Action spectra of the incident photon-to-current

conversion efficiencies (IPCE) as a function of incident wavelength for the quasi-solid-state DSSCs are shown in Fig. 7. It can be found that **FNE60** based quasi-solid-state DSSC displays a maximum IPCE of 75%. Upon the incorporation of an auxiliary EDOT unit into the π-conjugation bridge, the DSSC based on sensitizer **FNE62** exhibits a increased IPCE maximum of 85% along with significantly expanded photo-response range, which is obviously due to the bathochromic shift of the maximum absorption band of **FNE62** loaded TiO_2 film compared with that for **FNE60**. However, replacing the cyanoacrylic acid in sensitizers **FNE60** and **FNE62** with rhodanine-3-acetic acid group, the quasi-solid-state DSSCs based on both **FNE61** and **FNE63** display much lower IPCE values with maximum below 50%. According to the formula (2):[31]

$$IPCE(\lambda) = LHE(\lambda) \times \Phi_{inj} \times \Phi_c \qquad (2)$$

where LHE(λ) is the light-harvesting efficiency, Φ_{inj} is the electron injection efficiency, and Φ_c is the charge collection efficiency, since the LHE for the dye-loaded 15 μm thick TiO_2 film is close to unity for all the three devices, the relative low IPCE values for the DSSCs based on **FNE61** and **FNE63** are probably due to the low electron injection efficiency or charge collection efficiency. Although the driving force for the electron injection is sufficient, the methylene group interrupts the LUMO delocalization over the carboxylic acid, as revealed by the theoretic calculation, which reduces the electron injection efficiency or the charge collection efficiency and therefore dramatically lowers down the IPCE values. Compared with the IPCE spectrum of **FNE61** based quasi-solid-state DSSC, the DSSC based on **FNE63** displays a much broader IPCE spectrum obviously due to its bathochromic shift in the absorption spectrum (Fig. 3). It can be concluded that the quasi-solid-state DSSCs based on sensitizers **FNE62** and **FNE63** with D-π-A'-π-A configuration exhibit much wider photo-response range than those for the DSSCs based on **FNE60** and **FNE61** with D-A'-π-A configuration, respectively, which is beneficial to the photocurrent generation and power conversion efficiency.

Table 4 Photovoltaic performance of the quasi-solid-state DSSCs based on the four sensitizers.

Sensitizer	V_{oc} mV	J_{sc} mA cm^{-2}	FF %	η %
FNE60	656	13.97	67	6.1
FNE61	620	9.23	68	3.9
FNE62	682	17.59	68	8.2
FNE63	641	10.81	70	4.9

The photovoltaic performance of the quasi-solid-state DSSCs were evaluated under 100 mW cm^{-2} simulated AM 1.5 G solar light and the *J-V* curves are displayed in Fig. 8. The quasi-solid-state DSSC based on **FNE60** produces a J_{sc} of 13.97 mA cm^{-2} (Table 4). Upon the incorporation of an additional EDOT unit, sensitizer **FNE62** based DSSC provides an improved J_{sc} of 17.59 mA cm^{-2}, which is higher than the J_{sc} value (15.68 mA cm^{-2}) for **FNE46** based quasi-solid-state DSSC[12k] owning to the expanded photo-response range (Fig. 7). However, when the cyanoacrylic acid is replaced by rhodanine-3-acetic acid, although the absorption spectra of sensitizers **FNE61** and **FNE62** are broadened in comparison to those for sensitzers **FNE60** and **FNE62**, respectively, the quasi-solid-state DSSCs based on **FNE61** and **FNE63** produce a significantly decreased J_{sc} of 9.23 and 10.81 mA cm^{-2}, respectively. The J_{sc} values exhibit an order of **FNE61** < **FNE63** < **FNE60** < **FNE62**, which is consistent with the trend of the photo-

generated current integrated from the IPCE spectra (Fig. 7). Correspondingly, the quasi-solid-state DSSCs based on sensitizers **FNE60**, **FNE61**, **FNE62**, and **FNE63** offered a V_{oc} of 656, 620, 682, and 641 mV, respectively, and a *FF* of 67%, 68%, 68%, and 70%, respectively, corresponding to an η of 6.1%, 3.9%, 8.2%, and 4.9%, respectively.
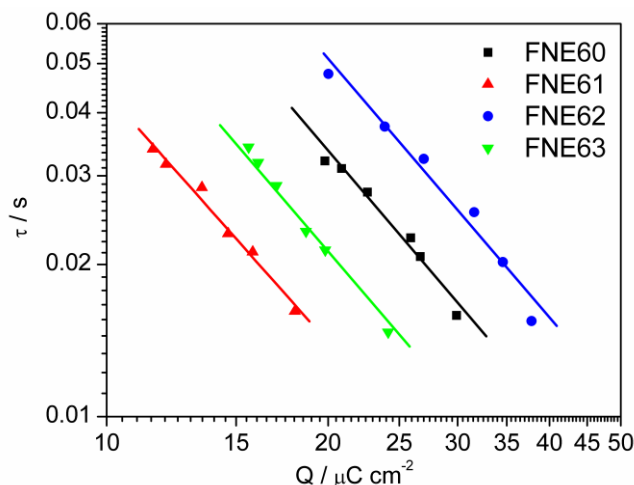
Fig. 9 Electron lifetime as a function of electron density at open circuit for the quasi-solid-state DSSCs.
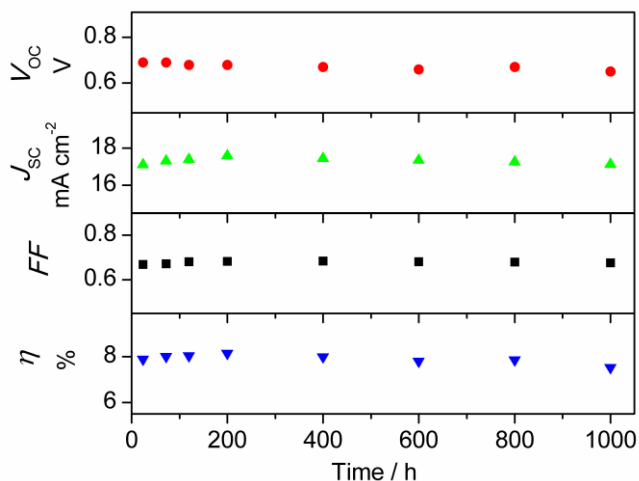
Fig. 10 Evolutions of photovoltaic performance parameters for **FNE62** based quasi-solid-state DSSC during one sun soaking.

To further qualitatively investigate the V_{oc} difference among the quasi-solid-state DSSCs, electron lifetime[32] against charge density[33] was evaluated since V_{oc} is related to the charge recombination rate in DSSCs while electron lifetime is a judgment for the charge recombination of injected electrons with I_3^- in the electrolyte at open-circuit. The electron lifetime (τ) was calculated by equation (3):[34]

$$\tau = (2\pi f_{min})^{-1} \qquad (3)$$

where f_{min} is the frequency at the top of the semicircle (f_{min}) measured by intensity modulated photovoltage spectroscopy (IMVS).[35] Fig. 9 shows the electron lifetimes of the quasi-solid-state DSSCs based on the four organic dyes as a function of Q. It can be found that for all the quasi-solid-state DSSCs, electron lifetime decreases with increasing Q. At a fixed Q, the electron

lifetime increases in the order of **FNE61** < **FNE63** < **FNE60** < **FNE62**, which is consistent with the V_{oc} trend shown in Fig. 8. The relatively shorter electron lifetimes for the DSSCs based on sensitizers **FNE61** and **FNE63** with rhodanine-3-acetic acid as anchoring group may be due to the poor electron injection efficiency which has a negative effect on the competition process between the circuit current and dark current.[28a] Since a retarded charge recombination rate constant can reduce electron loss at open circuit, more charge is accumulated in TiO₂. As a result, Fermi level moves upward and the V_{oc} values for the DSSCs based on **FNE60** and **FNE62** with cyanoacrylic acid groups get larger than those for the DSSCs based on **FNE61** and **FNE63** with rhodanine-3-acetic acid groups.

Finally, the stability of the quasi-solid-state DSSCs based on the resulting sensitizers was recorded over a period of 1000 h under one sun soaking. Fig. 10 displays the photovoltaic performance parameters of sensitizer **FNE62** based quasi-solid-state DSSC under sunlight soaking. It can be found that the J_{sc}, V_{oc}, *FF*, and η values slightly changed within 5% of the initial value after 1000 h of one sun soaking, which indicates that the quasi-solid-state DSSC based on sensitizer **FNE62** demonstrates good long-term stability.

Conclusions

In summary, four novel organic sensitizers with different numbers of EDOT bridge and different anchoring groups have been designed and synthesized. Either the incorporation of an auxiliary EDOT unit into sensitizer **FNE60** with D-A'-π-A configuration, or the replacement of thiophene bridge in sensitizer **FNE46** by EDOT unit, sensitizer **FNE62** with D-π-A'-π-A configuration illustrates a much broader absorption spectrum, which contributes to the light-harvesting property and photocurrent generation. Further strengthened ICT interactions and bathochromically shifted absorption maxima can be achieved by introducing rhodanine-3-acetic acid instead of cyanoacrylic acid in sensitizers **FNE60** and **FNE62**. However, the quasis-olid-state DSSCs based on sensitizers **FNE61** and **FNE63** demonstrate less effective electron injection from the excited dye molecules to the titania semiconductor due to the interruption of the LUMO delocalization on the carboxylic acid by the methylene group. Therefore, the quasi-solid-state DSSC based on sensitizer **FNE62** displays the highest power conversion efficiency of 8.2%, which exhibits good long-term stability after continuous light soaking.

Notes and references

Lab of Advanced Materials & Department of Chemistry, Collaborative Innovation Center of Chemistry for Energy Materials, Fudan University, Shanghai 200438, P. R. China. E-mail: zhougang@fudan.edu.cn.

1   O'Regan and M. Grätzel, *Nature*, 1991, **353**, 737.
2   (a) M. K. Nazeeruddin, A. Kay, I. Rodicio, R. Humphry-Baker, E. Mueller, P. Liska, N. Vlachopoulos and M. Grätzel, *J. Am. Chem. Soc.*, 1993, **115**, 6382; (b) M. K. Nazeeruddin, F. D. Angelis, S. Fantacci, A. Selloni, G. Viscardi, P. Liska, S. Ito, B. Takeru and M. Grätzel, *J. Am. Chem. Soc.*, 2005, **127**, 16835.

This journal is © The Royal Society of Chemistry 2014

J. Mater. Chem. A, 2014, **2**, 1-11 | 9

3   M. K. Nazeeruddin, P. Péchy, T. Renouard, S. M. Zakeeruddin, R. Humphry-Baker, P. Comte, P. Liska, L. Cevey, E. Costa, V. Shklover, L. Spiccia, G. B. Deacon, C. A. Bignozzi and M. Grätzel. *J. Am. Chem. Soc.*, 2001, **123**, 1613.

4   (a) A. Yella, H. W. Lee, H. N. Tsao, C. Yi, A. K. Chandiran, M. K. Nazeeruddin, E. W. G. Diau, C. Y. Yeh, S. M. Zakeeruddin and M. Grätzel, *Science*, 2011, **334**, 629; (b) L.-L. Li and E. W.-G. Diau, *Chem. Soc. Rev.*, 2013, **42**, 291; (c) A. Yella, C.-L. Mai, S. M. Zakeeruddin, S.-N. Chang, C.-H. Hsieh, C.-Y. Yeh and M, Grätzel, *Angew. Chem. Int. Ed.*, 2014, **53**, 2973; (d) S. Fan, K. Lv, H. Sun, G. Zhou, and Z.-S. Wang, *J. Power Sources*, 2015, **279**, 36.

5   S. Mathew, A. Yella, P. Gao, R. Humphry-Baker, F.E. Curchod, N. Ashari-Astani, I. Tavernelli, U. Rothlisberger, M. K. Nazeeruddin and M. Grätzel, *Nature Chem.*, 2014, **6**, 242.

6   (a) A. Mishra, M. K. R. Fischer and P. Bäuerle, *Angew. Chem. Int. Ed.*, 2009, **48**, 2474; (b) M. Liang and J. Chen, *Chem. Soc. Rev.*, 2013, **42**, 3453; (c) Y. Wu and W. Zhu; *Chem. Soc. Rev.*, 2013, **42**, 2039.

7   (a) M. Zhang, Y. Wang, M. Xu, W. Ma, R. Li and P. Wang, *Eergy Environ. Sci.*, 2013, **6**, 2944; (b) K. Kakiage, Y. Aoyama, T. Yano, T. Otsuka, T. Kyomen, M. Unno and M. anaya, *Chem. Commun.*, 2014, **50**, 6379.

8   (a) P. Wang, S. M. Zakeeruddin, J. E. Moser, M. K. Nazeeruddin, T. Sekiguchi and M. Grätzel, *Nat. Mater.*, 2003, **2**, 402; (b) Y. Shibata, T. Kato, T. Kado, R. Shiratuchi, W. Takashima, K. Kanetoa and S. Hayase, *Chem. Commun.*, 2003, **39**, 2730; (c) J.-J.Kim, H. Choi, J.-W. Lee, M.-S. Kang, K. Song, S. O. Kang and J. Ko, *J. Mater. Chem.*, 2008, **18**, 5223; (d) H. Tian, X. Jiang, Z. Yu, L. Kloo, A. Hagfeldt, and L. Sun，*Angew. Chem. Int. Ed.*, 2010, **49**, 7328; (e) Z. Yu, D. Qin, Y. Zhang, H. Sun, Y. Luo, Q. Meng and D. Li, *Energy Environ. Sci.*, 2011, **4**, 1298; (g) H. Wang, X. Zhang, F. Gong, G. Zhou and Z.-S. Wang, *Adv. Mater.,* 2012, **24**, 121; (g) Y. Shi, C. Zhu, L Wang, C. Zhao, W. Li, K. K. Fung, T. Ma, A. Hagfeldt and N. Wang, *Chem. Mater.*, 2013, **25**, 1000.

9   Q. Feng, X. Jia, G. Zhou and Z.-S. Wang, *Chem. Commun.*, 2013, **49**, 7445

10   (a) M. Velusamy, K. R. J. Thomas, J. T. Lin, Y. C. Hsu and K. C. Ho, *Org. Lett.*, 2005, **7**, 1899; (b) Y. Wu, X. Zhang, W. Li, Z.-S. Wang, H. Tian and W. Zhu, *Adv. Energy Mater.*, 2012, **2**, 149; (c) D. H. Lee, M. J. Lee, H. M. Song, B. J. Song, K. D. Seo, M. Pastore, C. Anselmi, S. Fantacci, F. De Angelis, M. K. Nazeeruddin, M. Grätzel and H. K. Kim, *Dyes Pigm.*, 2011, **91**, 192; (d) J. Kim, H. Choi, J. Lee, M. Kang, K. Song, S. O. Kang and J. Ko, *J. Mater. Chem.*, 2008, **18**, 5223; (e) Z. M. Tang, T. Lei, K. J. Jiang, Y. L. Song and J. Pei, *Chem. -Asian J.*, 2010, **5**, 1911; (f) S. Haid, M. Marszalek, A. Mishra, M. Wielopolski, J. Teuscher, M. Ros. Humphry-Baker, S. M. Zakeeruddin, M. Grätzel and P. Bäuerle, *Adv. Funct. Mater.*, 2012, **22**, 1291; (g) Y. Z. Wu, M. Marszalek, S. M. Zakeeruddin, Q. Zhang, H. Tian, M. Grätzel and W. H. Zhu, *Energy Environ. Sci.*, 2012, **5**, 8261; (h) S. Cai, X. Hu, Z. Zhang, J. Su, X. Li, A Islam, L. Han, H. Tian, *J. Mater. Chem. A*, 2013, **1**, 4763; (i) A Yella, C.-L. Mai, S. M. Zakeeruddin, S.-N. Chang, C.-H. Hsieh, C.-Y. Yeh, M. Grätzel, *Angew. Chem. Int. Ed.*, 2014, **53**, 2973.

11   (a) S. Qu, W. Wu, J. Hua, C. Kong, Y. Long and H. Tian, *J. Phys. Chem. C*, 2010, **114**, 1343; (b) S. Y. Qu, B. Wang, F. Guo, J. Li, W. Wu, C. Kong, Y. Long and J. Hua, *Dyes Pigm.*, 2012, **92**, 1384; (c) S. Qu, C. Qin, A. Islam, Y. Wu, W. Zhu, J. Hua, H. Tian and L. Han, *Chem. Commun.*, 2012, **48**, 6972; (d) J. Warnan, L. Favereau, Y. Pellegrin, E. Blart, D. Jacquemin and F. Odobel, *J. Photochem. Photobiol. A*, 2011, **226**, 9; (e) F. Guo, S. Qu, W. Wu, J. Li, W. Ying and J. Hua, *Synth. Met*., 2010, **160**, 1767; (f) L. Favereau, J. Warnan, F. B. Anne, Y. Jacquemin, F. Odobel, *J. Mater. Chem. A*, 2013, **1**, 7572; (g) F. Zhang, K.-J. Jiang, J.-H. Huang, C.-C. Yu, S.-G. Li, M.-G. Chen, L.-M. Yang and Y.-L. Song, *J. Mater. Chem. A*, 2013, **1**, 4858.

12   (a) D. W. Chang, H. J. Lee, J. H. Kim, S. Y. Park, S.-M. Park, L. Dai and J.-B. Baek, *Org.Lett*., 2011, **13**, 3880; (b) S.-R. Li, C.-P. Lee, H.-T. Kuo, K.-C. Ho and S.-S. Sun, *Chem. Eur. J.*, 2012, **18**, 12085; (c) J. Shi, J. Chen, Z. Chai, H. Wang, R. Tang, K. Fan, M. Wu, H. Han, J. Qin, T. Peng, Q. Li and Z. Li, *J. Mater. Chem.*, 2012, **22**, 18830; (d) K. Pei, Y. Wu, W. Wu, Q. Zhang, B. Chen, H. Tian and W. Zhu, *Chem. Eur. J.*, 2012, **18**, 8190; (e) K. Pei, Y. Wu, A. Islam, Q. Zhang, L. Han,

H. Tian and W. Zhu, *ACS Appl. Mater. Interfaces*, 2013, **5**, 4986; (f) H. Li, T. M. Koh, A. Hagfeldt, M. Grätzel, S. G. Mhaisalkar and A. C. Grimsdale, *Chem. Commun*., 2013, **49**, 2409; (h) C. A. Richard, Z. Pan, A. Parthasarathy, F. A. Arroyave, L. A. Estrada, K. S. Schanze and J. R. Reynolds, *J. Mater. Chem. A*, 2014, **2**, 9866; (i) L.-P. Zhang, K.-J. Jiang, G. Li, Q.-Q. Zhang and L.-M. Yang, *J. Mater. Chem. A*, 2014, **2**, 14852; (j) X. Lu, X. Jia, Z.-S. Wang and G. Zhou, *J. Mater. Chem. A*, 2013, **1**, 9697; (k) X. Lu, Q. Feng, T. Lan, G. Zhou and Z.-S. Wang, *Chem. Mater*., 2012, **24**, 3179.

13   (a) J. Yang, P. Ganesan, J. Teuscher, T. Moehl, Y. J. Kim, C. Yi, P. Comte, K. Pei, T. W. Holcombe, M. K. Nazeeruddin, J. Hua, S. M. Zakeeruddin, H. Tian and M. Grätzel, *J. Am. Chem. Soc.*, 2014, **136**, 5722 (b) K. Pei, Y. Wu, A. Islam, S. Zhu, L. Han, Z. Geng and W. Zhu, *J. Phys. Chem. C*, 2014, **118**, 16552.

14   (a) G. Zhang, H. Bala, Y. Cheng, D. Shi, X. Lv, Q. Yu and P. Wang, *Chem. Commun.*, 2009, 2198; (b) M. Xu, S. Wenger, H. Bala, D. Shi, R. Li, Y. Zhou, S. M. Zakeeruddin, M. Grätzel and P. Wang, *J. Phys. Chem. C*, 2009, **113**, 2966; (c) Q. Yu, S. Liu, M. Zhang, N. Cai, Y. Wang and P. Wang, *J. Phys. Chem. C*, 2009, **113**, 14559; (d) G. Li, K.-J. Jiang, P. Bao, Y.-F. Li, S.-L. Li and L.-M. Yang, *New J. Chem.*, 2009, **33**, 868; (e) W. Zeng, Y. Cao, Y. Bai, Y. Wang, Y. Shi, M. Zhang, F. Wang, C. Pan and P. Wang, *Chem. Mater.*, 2010, **22**, 1915; (f) S. Wenger, P.-A. Bouit, Q. Chen, J. Teuscher, D. D Censo, R. Humphry-Baker, J.-E. Moser, J. L. Delgado, N. Martín, S. M. Zakeeruddin and M. Grätzel, *J. Am. Chem. Soc.*, 2010, **132**, 5164; (g) S. Paek, H. Choi, H. Choi, C.-W. Lee, M.-S. Kang, K. Song, M. K. Nazeeruddin and J. Ko, *J. Phys. Chem. C*, 2010, **114**, 14646; (h) J.-Y. Li, C.-Y. Chen, C.-P. Lee, S.-C. Chen, T.-H. Lin, H.-H. Tsai, K.-C. Ho and C.-G. Wu, *Org. Lett.*, 2010, **12**, 5454; (i) M. Liang, M. Lu, Q.-L. Wang, W.-Y. Chen, H.-Y. Han, Z. Sun and S. Xue, *J. Power Sources*, 2011, **196**, 1657; (j) B.-S. Chen, D.-Y. Chen, C.-L. Chen, C.-W. Hsu, H.-C. Hsu, K.-L. Wu, S.-H. Liu, P.-T. Chou and Y. Chi, *J. Mater. Chem.*, 2011, **21**, 1937; (k) Y. J. Chang and T. J. Chow, *J. Mater. Chem.*, 2011, **21**, 9523; (l) M.-H. Tsao, T.-Y. Wu, H.-P. Wang, I-W. Sun, S.-G. Su, Y.-C. Lin and C.-W. Chang, *Mater. Lett.*, 2011, **65**, 583; (m) S. H. Kim, H. W. Kim, C. Sakong, J. Namgoong, S. W. Park, M. J. Ko, C. H. Lee, W. I. Lee and J. P. Kim, *Org. Lett.*, 2011, **13**, 5784; (n) X. Cheng, M. Liang, S. Sun, Y. Shi, Z. Ma, Z. Sun, S. Xue, *Tetrahedron*, 2012, **68**, 5375; (o) L. Cai, H. N. Tsao, W. Zhang, L. Wang, Z. Xue, M. Grätzel and B. Liu, *Adv. Energy Mater.*, 2013, **3**, 200; (p) N. Cai, Y. Wang, M. Xu, Y. Fan, R. Li, M. Zhang and P. Wang, *Adv. Funct. Mater.*, 2013, **23**, 1846; (q) Q. Feng, X. Jia, G. Zhou and Z.-S. Wang, *Chem. Commun.*, 2013, **49**, 7445; (r) M.-W. Lee, J.-Y. Kim, D.-H. Lee and M. J. Ko, *ACS Appl. Mater. Interfaces* 2014, **6**, 4102.

15   (a) T. Horiuchi, H. Miura and S. Uchida, *Chem. Commun.*, 2003, 3036; (b) T. Horiuchi, H. Miura, K. Sumioka and S. Uchida, *J. Am. Chem. Soc.*, 2004, **126**, 12218; (c) S. Ito, S. M. Zakeeruddin, R. Humphry-Baker, P. Liska, R. Charvet, P. Comte, M. K. Nazeeruddin, P. Péchy, M. Takata, H. Miura, S. Uchida and M. Grätzel, *Adv. Mater.*, 2006, **18**, 1202; (d) M. Liang, W. Xu, F. Cai, P. Chen, B. Peng, J. Chen and Z. Li, *J. Phys. Chem. C*, 2007, **111**, 4465; (e) S. Ito, H. Miura, S. Uchida, M. Takata, K. Sumioka, P. Liska, P. Comte, P. Péchy and M. Grätzel, *Chem. Commun.*, 2008, **5194**; (f) H. Tian, X. Yang, R. Chen, A. Hagfeldt and L. Sun, *Energy Environ. Sci.*, 2009, **2**, 674; (g) J. Wiberg, T. Marinado, D. P. Hagberg, L. Sun, A. Hagfeldt and B. Albinsson, *J. Phys. Chem. C*, 2009, **113**, 3881; (h) H.-M. Cheng and W.-F. Hsieh, *Energy Environ. Sci.*, 2010, **3**, 442; (i) W. Li, Y. Wu, X. Li, Y.Xie and W. Zhu, *Energy Environ. Sci.*, 2011, **4**, 1830; (j) J. Mao, N. He, Z. Ning, Q. Zhang, F. Guo, L. Chen, W. Wu, J. Hua and H. Tian, *Angew. Chem.* 2012, **124**, 10011; (k) M. Matsui, T. Shiota, Y. Kubota, K. Funabiki, J. Jin, T. Yoshida, S. Higashijima and H. Miura, *Tetrahedron*, 2012, **68**, 4286; (l) G. Wu, F. Kong, J. Li, X. Fang, Y. Li, S. Dai, Q. Chen and X. Zhang, *J. of Power Sources*, 2013, **243**, 131; (m) K. Rakstys, J. Solovjova, T. Malinauskas, I. Bruder, R. Send, A. Sackus, R. Sens, V. Getautis, *Dyes and Pigments*, 2014, **104**, 211; (n) C. A. Echeverry, A. Insuasty, M. Á. Herranz, A. Ortí, R. Cotta, V. Dhas, L. Echegoyen, B. Insuasty, N. Martín, 2014, **104**, 9; (o) V. Dryza and E. J. Bieske, *J. Phys. Chem. C*, 2014, **118**, 19646; (p) C. A. Echeverry, M. A. Herranz, A. Ortiz, B. Insuasty and N. Martín, *New J.*

C hem., 2014, **38**, 5801; (q) J. Zhao, X. Yang, M. Cheng, W. Wang and L. Sun, *RSC Adv.*, 2014, **4**, 4811; (r) D. Arteaga, R. Cotta, A. Ortiz, B. Insuasty, N. Martin, L. Echegoyen, *Dyes and Pigments*, 2015, **112**, 127.

16 N. Blouin, A. Michaud, D. Gendron, S. Wakim, E. Blair, R. Neagu-Plesu, M. Belletête, G. Durocher, Y. Tao, and M. Leclerc, *J. Am. Chem. Soc.*, 2008, **130**, 732.

17 T. Taerum, O. Lukoyanova, R. G. Wylie and D. F. Perepichka, *Org. Lett.*, 2004, **6**, 273.

18 D. Milstein and J. K. Stille, *J. Am. Chem. Soc.*, 1978, **100**, 3636.

19 (a) V. J. Majo and P. J. Perumal, *J. Org. Chem.*, 1996, **61**, 6523; (b) O. Meth-Cohn and M. Ashton, *Tetrahedron Lett.*, 2000, **41**, 2749.

20 N. Miyaura and A. Suzuki, *Chem. Rev.*, 1995, **95**, 2457.

21 V. J. Majo, and P. J. Perumal, *J. Org. Chem.*, 1996, **61**, 6523

22 W. Zhu, Y. Wu, S. Wang, W. Li, X. Li, J. Chen, Z.-S. Wang and H. Tian, *Adv. Funct. Mater.*, 2011, **21**, 756.

23 L. Cai, H. Tsao, W. Zhang, L. Wang, Z. Xue, M. Grätzel and B. Liu, *Adv. Energy Mater.*, 2012, **3**, 200.

24 A. Hagfeldt and M. Grätzel, *Chem. Rev.*, 1995, **95**, 49.

25 Z.-S. Wang, N. Koumura, Y. Cui, M. Takahashi, H. Sekiguchi, A. Mori, T. Kubo, A. Furube and K. Hara, *Chem. Mater.*, 2008, **20**, 3993

26 A. Hagfeldt, G. Boschloo, L. Sun, L. Kloo and H. Pettersson, *Chem. Rev.*, 2010, **110**, 6595.

27 M. J. Frisch, G. W. Trucks, H. B. Schlegel, G. E. Scuseria, M. A. Robb, J. R. Cheeseman, J. A. Montgomery, T. Vreven, K. N. Kudin, J. C. Burant, J. M. Millam, S. S. Iyengar, J. Tomasi, V. Barone, B. Mennucci, M. Cossi, G. Scalmani, N. Rega, G. A. Petersson, H. Nakatsuji, M. Hada, M. Ehara, K. Toyota, R. Fukuda, J. Hasegawa, M. Ishida, T. Nakajima, Y. Honda, O. Kitao, H. Nakai, M. Klene, X. Li, J. E. Knox, H. P. Hratchian, J. B. Cross, V. Bakken, C. Adamo, J. Jaramillo, R. Gomperts, R. E. Stratmann, O. Yazyev, A. J. Austin, R. Cammi, C. Pomelli, J. W. Ochterski, P. Y. Ayala, K. Morokuma, G. A. Voth, P. Salvador, J. J. Dannenberg, V. G. Zakrzewski, S. Dapprich, A. D. Daniels, M. C. Strain, O. Farkas, D. K. Malick, A. D. Rabuck, K. Raghavachari, J. B. Foresman, J. V. Ortiz, Q. Cui, A. G. Baboul, S. Clifford, J. Cioslowski, B. B. Stefanov, G. Liu, A. Liashenko, P. Piskorz, I. Komaromi, R. L. Martin, D. J. Fox, T. Keith, M.A. Al-Laham, C.Y. Peng, A. Nanayakkara, M. Challacombe, P. M. W. Gill, B. Johnson, W. Chen, M. W. Wong, C. Gonzalez, J. A. Pople, *Gaussian 03*, Revision C.02, Gaussian, Inc., Wallingford, CT, 2004.

28 (a) H. Tian, X. Yang, R. Chen, R. Zhang, A. Hagfeldt and L. Sun, *J. Phys. Chem. C*, 2008, **112**, 11023; (b) W.-H. Liu, I-C. Wu, C.-H. Lai, C.-H. Lai, P.-T. Chou, Y.-T. Li, C.-L. Chen, Y.-Y. Hsu and Y. Chi, *Chem. Commun.*, 2008, 5152; (c) G. S. Kumar, K. Srinivas, B. Shanigaram, D. Bharath, S. P. Singh, K. Bhanuprakash, V. J. Rao, A. Islamd and L. Han, *RSC Adv.* 2014, **4**, 13172.

29 (a) D. Kuang, S. Ito, B. Wenger, C. Klein, J.-E Moser, R. H.-Baker, S. M. Zakeeruddin and M. Grätzel, *J. Am. Chem. Soc.*, 2006, **128**, 4146; (b) D. P. Hagberg, J.-H. Yum, H. Lee, F. D. Angelis, T. Marinado, K. M. Karlsson, R. H.-Baker, L. Sun, A. Hagfeldt, M. Grätzel and M. K. Nazeeruddin, *J. Am. Chem. Soc.*, 2008, **130**, 6259; (c) Z. Zhang, P. Chen, T. N. Murakami, S. M. Zakeeruddin and M. Grätzel, *Adv. Funct. Mater.*, 2008, **18**, 341; (d) S. Paek, H. Choi, C. Kim, N. Cho, S. So, K. Song, M. K. Nazeeruddin and J. Ko, *Chem. Commun.*, 2011, **47**, 2874; (e) A. Ehret, L. Stuhl and M. T. Spitler, *J. Phys. Chem. B*, 2001, **105**, 9960.

30 X. Lu, G. Zhou, H. Wang, Q. Feng and Z.-S. Wang, *Phys. Chem. Chem. Phys.*, 2012, **14**, 4802.

31 Y. Chiba, A. Islam, R. Komiya, N. Koide and L. Han, *Appl. Phys. Lett.,* 2006, **88**, 223505.

32 (a) M. Miyashita, K. Sunahara, T. Nishikawa, Y. Uemura, N. Koumura, K. Hara, A. Mori, T. Abe, E. Suzuki and S. Mori, *J. Am. Chem. Soc.*, 2008, **130**, 17874; (b) B. O'Regan, K. Walley, M. Juozapavicius, A. Anderson, F. Matar, T. Ghaddar, S. M. Zakeeruddin, C. Klein and J. R. Durrant, *J. Am. Chem. Soc.*, 2009, **131**, 3541.

33 N. Kopidakis, N. R. Neale and A. J. Frank, *J. Phys. Chem. B*, 2006, **110**, 12485.

34 G. Schlichthorl, S. Y. Huang, J. Sprague and A. J. Frank, *J. Phys. Chem. B*, 1997, **101**, 8141.

35 N. W. Duffy, L. M. Peter, R. M. G. Rajapakse and K. G. U. Wijayantha, *J. Phys. Chem. B*, 2000, **104**, 8916.

This journal is © The Royal Society of Chemistry 2014

J. Mater. Chem. A, 2014, **2**, 1-11 | **11**

Table of Contents Entry

$A = $ (structures shown)
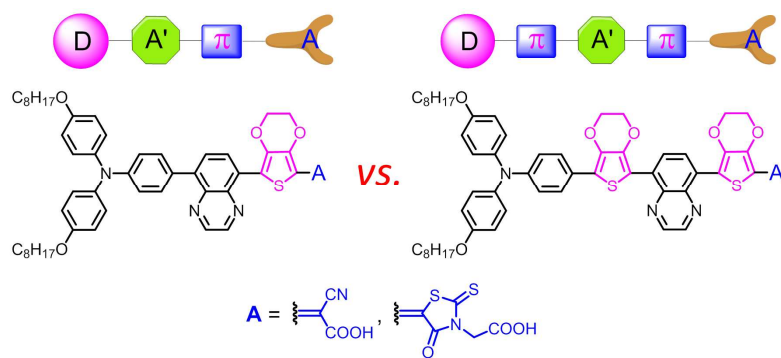
Four D-(π)-A'-π-A featured organic sensitizers with different building blocks have been constructed for efficient quasi-solid-state dye-sensitized solar cells.